Fluid flow characteristics for a diverging-converging magnetohydrodynamic electric current configuration.

Okey Oseloka Onyejekwe[1]

[1] Computational Science Program, Addis Ababa University Arat Kilo Campus Addis Ababa Ethiopia

Abstract

The effects of variations in flow field due to the presence of electromagnetic rotational forces on a transient incompressible and electrically conducting fluid flow are sought. These variations result from interactions between the electric currents with a nonuniform magnetic field. The governing equations are coupled and nonlinear and are discretized using the finite difference technique. Numerical results illustrating the development of secondary flows by the rotational electromagnetic force field are displayed, as well as the effects on the streamline axial velocity profiles by the magnetic pressure number and the flow Reynolds numbers.

Keywords: finite difference, secondary flows, magnetic pressure number, Reynolds number, coupled and nonlinear equations, electromagnetic pressure number.

NOMENCLATURE

$\bar{B}$	magnetic field
$\bar{E}$	electric field intensity
f	electromagnetic body force per unit volume
g	gravitational acceleration
h	magnetic field intensity
h_θ	component of the magnetic field intensity in the azimuthal direction
$\bar{j}$	current density
$\bar{j}_0$	reference current density
p	pressure
r	radial coordinate
r_0	reference coordinate

r_1 radius of aperture

r_2 radial distance from top of aperture to upper wall

R dimensionless radial coordinate

R_e Reynolds number

RB analog of streamlines for current flow

t time coordinate

u_z axial velocity

u_0 reference velocity

U dimensionless axial velocity

u_r radial velocity

V dimensionless radial velocity

z axial coordinate

Z dimensionless axial coordinate

Greek Symbols

∇ gradient

μ_m magnetic permeability of fluid medium

ν kinematic viscosity

ψ stream function

Ψ dimensionless stream function

ρ density

τ dimensionless time

$\bar{\omega}$ dimensionless vorticity

μ magnetic permeability

σ electrical conductivity

ζ = magnetic pressure number

Subscripts

i,j node counters in axial and radial directions

1. INTRODUCTION

Magnetohyroynamics (MHD) deals with the interaction between electrically-conducting fluids and applied electromagnetic fields. The coupling between the two fields results in some exciting physics among which are; the development of secondary flows due to the presence of rotational force fields, the development of electric current due to the interaction of the magnetic field and a conducting fluid, and the generation of the Lorentz force arising from the presence of a current and a magnetic field. The effect of this force is dynamical, because it acts on the conducting fluid and modifies its motion. The motion in turn modifies the field, which also modifies the motion.

The description of MHD flows involves the solution of the equations of fluid dynamics, the so called Navier-Stokes equations, and the equations of electrodynamics. These two equations are mutually coupled via the Lorentz force, and the Ohm's Law; hence it is useful to understand the influence of an externally generated body force on a conducting fluid in various dimensions for time dependent applications.

The conversion of electrical energy directly into a body force, defines the magnetohydrodynamic concept .Fundamental to this, is the interaction of an electromagnetic field and conducting fluid which may be gas or liquid . From a unified viewpoint, plasma physics can be considered a special case of magnetohydrodynamics because of its strong dependence on the kinetic theory fluid model, involving gases in the plasma regime. However for the purposes of this study, our emphasis will be concentrated more on the electromagnetic-fluid interaction model.

MHD has always attracted a keen research interest. The stimulus for much of this interest lies in the desire to further understand the influence of electric and magnetic fields on heat and momentum transfer as they affect fluid flow. There are a couple of applications of MHD that hold great potential for future use for example energy conversion devices, flight and energy control of space re-entry vehicles, nuclear fusion control, electricity generation, etc. In a coal-fired MHD power generator, gas produced by combusting coal expands through a nozzle and interacts with a magnetic field to produce electricity. The MHD power generator is beginning to take on an added importance because of the current global energy crisis and environmental pollution. A conducting fluid moves across a magnetic field and in the process generates electrical

energy which is tapped by making suitable connections to an external load . Some obvious advantages arising from this type of power generation include less pollution, and cheaper operational costs. Also, the reliable prediction of MHD flows coupled with strong magnetic fields is a key factor for the design of liquid metal blankets for use in fusion reactors.

It has been shown that the passage of electric current through a flowing conducting fluid radically alters the flow profile(Chow and Uberoi [1)]. Uberoi[2] adopted a linear analysis to study the effect of an axial current on the motion of an incompressible inviscid fluid through an insulated axisymmetric tube of varying cross-sectional area. The slowing down of the central flow when approaching the tube contraction was attributed to the electromagnetic pinch effect. For example, when draining a current-carrying fluid from the apex of a conical tube, only the fluid in the narrow region near the wall can go through the apex. The oncoming flow along the tube axis experiences rapid deceleration, that forces the fluid to become stagnant before reaching the throat (Narain and Uberoi[3]). This type of flow was found to result in recirculation downstream of the stagnation point.

Given the vast range of MHD applications and the variability of the dimensionless numbers involved; it is not possible to arrive at complete numerical or analytical solutions of the governing differential equations. Hence the challenge lies in developing both numerical and analytical techniques to deal with each problem depending on the physics and accompanying rigor.

The flow of conducting fluid in pipes in the presence of electromagnetic forces has been studied analytically by various authors. A good account of this can be found in Sherclif [4], Di Pizza and Buhler[5]. Uberoi and Chow[6] reported solutions for large scale motions in electrical discharges. Subsequent work on channel flow can be found in the thesis by Ritter[7],and the papers by Chamkha[8,9,10], Onyejekwe[11]. Pantokratoras[12], studied the fully developed flow between parallel plates in an electrically conducting fluid under the action of induced magnetic field for the case where both the magnetic and electric fields are situated on the lower plate. Making some reasonable assumptions, he obtained one-dimensional exact analytical solutions for the velocity, flow rate, and wall shear stress at the plates for weakly electrically conducting fluids. His results though restricted in scope, could be used as adequate starting point from more complex considerations of MHD flows. The application of MHD to microfluidic devices is another blossoming area of research. The magnetohydrodynamic (MHD) pumping provides an efficient, cheap, reliable and easily controllable method for pumping various liquids for the purposes of testing samples of blood, DNA and drugs in nano or microscales. Kabbani *et al.*[13] proposed approximate solutions for the velocity profile of steady incompressible MHD flows in a rectangular microchannel driven by

Lorentz force. Their solutions were found to compare favorably with existing computational and analytical results.

In the work reported herein, we present numerical solutions governing a laminar electrically conducting viscous fluid through a horizontal tube connected to an electrical field . Such an electrical field is created by applying potential differences across a couple of screen electrodes placed at different positions in the nonconducting tube (Fig. 1). We apply the no-slip boundary conditions at the bounding walls to track the vorticities generated by the rotational body forces as well those generated by the solid walls. Both the modification of the originally flow field by the rotational force field as well as the development of MHD flow at various stages are of primary interest as well as the influence of the magnetic pressure number on the development of secondary flows.

2. PROBLEM FORMULATION

We consider a circular tube with screen electrodes positioned at the entrance and middle of the tube. A conducting fluid can move freely through the end electrodes. Both of them are separated by the same distance z_0 from the center of the tube. The tube axis is at the center of the duct and its axis is parallel to the side wall and orthogonal to the streamwise direction [Fig. 1]. A converging and diverging current flow is obtained by applying potential differences across the electrodes. A coordinate system is used with the origin positioned at the center of the circular tube, and the coordinates r, and z are aligned respectively along the channel height and width. The channel surface can be taken as nonconducting. It is our goal to determine the flow and electromagnetic fields as well as secondary flows that can exist for this configuration, given the appropriate governing differential equations, initial and boundary conditions.

On the assumptions that (a) fluid flow is incompressible (b) the induced magnetic field is negligibly smaller than the applied magnetic field and hence much smaller than the total magnetic field **B** . This is because the magnetic Reynolds number is considered small. (c) Both the displacement current and the free charge density are also considered negligible. (d) The Lorenz force is the only body force on the fluid (e) the velocity of flow is regarded as too small compared to the velocity of light as a consequence of this relativistic effects are ignored. The governing differential equations of motion for an incompressible electrically conducting fluid in a tube can be expressed together with the Maxwell equations in the following form

When an electric current is passed through the conducting fluid, a magnetic field is generated and a current density **J** transmits through the fluid. Relativistic effects are

ignored for cases where the velocity of flow is small compared to the velocity of light. For steady state, even if the fluid were moving, the electromagnetic equations can be written in the form:

$$\frac{\partial \bar{u}}{\partial t} + \nabla \times (\bar{u} \bullet \nabla)\bar{u} = -\nabla\left(\frac{p}{\rho} + gr\right) + \nu\left(\nabla^2 \bar{u}\right) + \frac{\mu_m}{\rho}\left(\bar{j} \times \bar{B}\right) \qquad (1)$$

The curl of equation (1)

$$\nabla \times \frac{\partial \bar{u}}{\partial t} + \nabla \times (\bar{u} \bullet \nabla)\bar{u} = -\nabla \times \nabla\left(\frac{p}{\rho} + gr\right) + \nabla \times \left(\nu \nabla^2 \bar{u}\right) + \nabla \times \left[\left(\nabla \times \bar{B}\right) \times \bar{B}\right] \quad (2)$$

where

$$\left.\begin{aligned}
&\nabla \times \frac{\partial \bar{u}}{\partial t} = \frac{\partial}{\partial t}\left(\nabla \times \bar{u}\right) = \frac{\partial \bar{\omega}}{\partial t} \\
&\nabla \times (\bar{u} \bullet \nabla)\bar{u} = \nabla \times \nabla(\bar{u} \times u) - \nabla \times \left[u \times \left(\nabla \times \bar{u}\right)\right] \\
&\nabla\left(\bar{u} \bullet \bar{u}\right) = 2(\bar{u} \bullet \nabla)\bar{u} + 2\bar{u} \times \left(\nabla \times \bar{u}\right) \\
&\bar{u}(\bar{u} \bullet \nabla) = \frac{1}{2}\nabla\left(u^2\right) - (\bar{u} \times \bar{\omega}) \\
&\nabla \times (\bar{u} \times \nabla)\bar{u} = \nabla \times \nabla\left(\frac{u^2}{2}\right) - \nabla \times (\bar{u} \times \bar{\omega}) \\
&\nabla \times (\bar{u} \times \nabla)\bar{u} = -\nabla \times (\bar{u} \times \bar{\omega}) = \nabla \times (\bar{\omega} \times \bar{u}) \\
&\nabla \times \left[\nabla\left(\frac{p}{\rho} + gr\right)\right] = 0 \\
&\nabla \times \left(\nu \nabla^2 \bar{u}\right) = \nu \nabla^2 \left(\nabla \times \bar{u}\right) = \nu \nabla^2 \omega \\
&\nabla \times \left[\left(\nabla \times \bar{B}\right) \times \bar{B}\right] = \nabla \times \left(\bar{h} \times \bar{B}\right) = \left(\bar{B} \bullet \nabla\right)\bar{h} - \left(\bar{h} \bullet \nabla\right)\bar{B} + \bar{h}\left(\nabla \bullet \bar{B}\right) + \bar{B}\left(\nabla \bullet \bar{h}\right)
\end{aligned}\right\}$$

The system of Maxwell equations can be written in the form:

$$\mu \bar{j} = \nabla \times \bar{B},\ \nabla \bullet \bar{j} = 0, \nabla \times \bar{E} = -\frac{\partial \bar{B}}{\partial t},\ \nabla \bullet \bar{B} = 0$$

Ohm's law can be written as:

$$\bar{j} = \sigma\left(\bar{E} + \mu \bar{u} \times \bar{B}\right) \qquad (3)$$

The body force term or the Lorentz force is given by: $\bar{f} = \bar{j} \times \mu_m \bar{B}$. It not only represents the force per unit volume that accounts for the coupling between the fluid

motion and the magnetic field, but also contributes in no small measure to the interesting physics of MHD flows.

Passage of electric current through a fluid will set the fluid in motion since in general, the potential; pressure forces can not be balanced by the rotational electromagnetic forces. Because of the axisymmetric geometry of tubular flow, the streamfunction can be utilized to satisfy the continuity equation, and is expressed as

$$u_z = \frac{1}{r}\frac{\partial \psi}{\partial r}, \quad u_r = -\frac{1}{r}\frac{\partial \psi}{\partial z} \qquad (4)$$

After carrying out the chores for nondimensionalization, the governing equations are given as:

$$U = \frac{1}{R}\frac{\partial \psi}{\partial R}, \; V = -\frac{1}{R}\frac{\partial \psi}{\partial R} \qquad (5a)$$

$$\left(\frac{\partial^2 \psi}{\partial R^2} - \frac{1}{R}\frac{\partial \psi}{\partial R} + \frac{\partial^2 \psi}{\partial R^2}\right)\frac{1}{R} = \omega \qquad (5b)$$

$$\left(\frac{\partial^2 \psi}{\partial R^2} - \frac{1}{R}\frac{\partial \psi}{\partial R} + \frac{\partial^2 \psi}{\partial R^2}\right) RB = 0 \qquad (5c)$$

$$\frac{\partial \omega}{\partial t} + \frac{\partial (U\omega)}{\partial Z} + \frac{\partial (V\omega)}{\partial R} = \zeta \frac{B}{R}\frac{\partial B}{\partial Z} + \frac{1}{\mathrm{Re}}\left(\frac{\partial^2 \omega}{\partial R^2} + \frac{1}{R}\frac{\partial \omega}{\partial R} - \frac{\omega}{R^2} + \frac{\partial^2 \omega}{\partial Z^2}\right) \qquad (5d)$$

An upwind scheme is used to handle the nonlinear convection terms in equation (5d). It would seem as if the computational overhead associated with the governing equations will be quite intense, however the computational rigor is simplified if we take into consideration the symmetrical nature of the electromagnetic flow and find the solution in the region $(-z_0 \le z \le 0)$ to the left of the central electrode and use the mirror image for the right of the electrode. This however does not apply to a net flow through the tube where the whole geometry is considered because the flow pattern should not be symmetric about a center point.

Our first consideration, involves the fluid dynamics of an unsteady flow of an electrically conducting viscous fluid through orifices positioned on the left and right hand sides ($z = \pm 1$) of an insulated tube (Fig.1) . The tube openings at the left and the tight sides are positioned at

distances $0.2r_0$ from the centerline. No-slip boundary conditions are set up at the tube walls, and by assuming that the flow is purely axial, we impose a zero perpendicular velocity (V=0) at entrance and exit. Boundary conditions for the stream functions comprise, $\psi = 0$ along the tube axis, and along the wall $\psi = 1/2$, at the entrance and exit $\partial\psi/\partial Z = 0$ respectively. We assume uniform flow through the tube axis. As a consequence, the axial velocity in this region is specified as: $U_{i,1} = 2\psi_{i,2}/h^2$.

Equations (5a) and (5b) as defined by the conservation of mass, show a similarity between the electromagnetic flow term RB and the stream function ψ. This allows for constant values of RB to behave like streamfunction. At the tube centerline and top wall, RB = 0, and RB=0.5 respectively. For the centrally placed electrode, $0 < R < r_1/r_0$, $\partial(RB)/\partial Z = 0$, and for $r_1/r_0 \le R \le -r_1/r_0$ RB=0.5 and at the left orifice $Z = -z_0/r_0$, $\partial(RB)/\partial Z = 0$. Vorticity is specified at zero at the walls as well its derivative with respect to the horizontal direction at the entrance and exit are both given zero values.

To set up the initial flow conditions, uniform flow for a unit axial velocity is assumed. The fluid can not remain stationary in the presence of a rotational electromagnetic body force and a predominantly axial motion is motivated by an electromagnetic force per unit volume $\mathbf{f} = \mu_m \mathbf{B}$ set up in the tube. It should be noted that the this body force is rotational and can not be balanced by viscous forces unless at steady state

The numerical strategy for solving this problem are enumerated as follows:

Non dimensional electrode and radial sizes of $r_1/r_0 = 0.1$, *and* $z_0/r_0 = 1$ together with a spatial increment of h= 0.1 are chosen. The governing differential equations are replaced by appropriate difference equations. Time and spatial coordinates are approximated by forward differencing in time and central differencing in space. Iterative procedures are adopted to approximate equations (5b) , (5c) and (5d). Two additional grid lines at the entrance and exit are deployed to handle derivative boundary conditions. The unsteady nonlinear equations together with the given boundary conditions are solved using an implicit, iterative finite difference scheme similar to the one described in Soundalgekar et al.[14].Square meshes are chosen to cover the problem domain. Since the absolute dimensionless distance between the central electrode and the inlet or exit is unity, the each grid has a value of $1/(n-1)$. After a series of trial, a 21x11 grid was chosen for computation for a time step $\Delta\tau = 0.01$.

$R\mathbf{B}$ is computed by solving equation (5c) iteratively to satisfy the boundary conditions. The $R\mathbf{B}$ scalar field gives us an idea of the 'streamlines of the current flow' in the problem domain. Having obtained $R\mathbf{B}$, the influence of the Lorentz force on the conducting fluid is determined

by computing the source term $\left(\zeta \frac{\mathbf{B}}{R}\frac{\partial \mathbf{B}}{\partial Z}\right)$ in equation(5d) for all interior grid points, where the magnetic pressure number is given as :

$$\zeta = \mu_m r_{r_0}^2 J_0^2 \big/ 1/2\rho u_0^2$$

The flow profile is determined by assuming a uniform flow of unit dimensionless speed and integrating equation (5a) for all the grid points. Since the flow field unlike the electromagnetic filed is not symmetrical, we have to pay due cognizance to the boundary conditions at the two ends of the tube containing the orifices. At any instant in time, the velocity and vorticity distributions are obtained from the conditions at the previous time step, eventhough at the beginning, they are obtained from a prescribed initial conditions. Streamfunction are computed based on the vorticity distribution by solving equation(5b). Velocity components are computed based on equation (5a) once the values of the streamfunction are known. These are again used to determine the vorticity field in the interior region for the next time step; and their boundary values updated appropriately. The same process is repeated at each of the time steps until the time counter reaches an apriorily specified value of maximum time or the computed scalar field satisfies the criterion for steady state. Our numerical results will then represent steady state profiles induced by an unsteady converging-diverging current field .

A second numerical experimentation involves replacing the orifices with two large screen electrodes covering the ends of the nonconducting tube. The governing equations for the electromagnetic field and the flow are the same, but appropriate changes are made to the boundary conditions to reflect the new configuration. Just like in the first example, the electromagnetic field is symmetrical about the central electrode so it is computed half the horizontal direction of the nonconducting tube and then reflected on the other side. Dirichlet boundary conditions of 0 and 0.5 Are specified for the tube centerline which constitutes the lower boundary as well as the top of the nonconducting tube. This amounts to setting up an electromagnetic barrier to the flow. We assume that the electromagnetic flow through the central electrode is purely horizontal, this is defined by setting up a Neumann or zero flux boundary condition at this point i.e. $\partial\left(R\mathbf{B}\right)\big/\partial Z = 0$. To guarantee that continuity requirements are satisfied, the total current through the central electrode (i.e. from its top the top of the tube) should be 0.5. Lastly in order to ensure that the electromagnetic field through the central electrode should be purely horizontal, a Neuman boundary condition is imposed on the left screen electrode ($\partial\left(R\mathbf{B}\right)\big/\partial Z = 0$)

Since the stream function ψ is the analog of $R\mathbf{B}$ by virture of equations (5b) and (5c), their boundary conditions are essentially the same except that for the flow boundary conditions care must be taken to reflect the fact the flow pattern is no longer symmetrical and hence must have to be specified for the entire problem domain. Since the stream function essentially represents

the volume of fluid per unit time between a given point and a reference plane, it is given values of 0 and 0.5 at the tubes lower boundary (the centerline) and the top boundary. The vorticity is set to zero at all boundaries. Axial flow through the end electrodes is guaranteed by setting the derivatives of the stream function and vorticity equal to zero $\left(\partial\psi/\partial Z=\partial\omega/\partial Z=0\right)$. This last equation, in combination with equations (5a) and (5b) determine the entire flow field (the radial and axial velocity components) in the problem geometry. For example at the centerline flow is purely axial and $\psi=0\Rightarrow V=0$. At the top wall $\psi=1/2\Rightarrow\partial\psi/\partial R=0$, in terms of the velocity components $V=0,\ \partial U/\partial R=0$ at the top wall. For the two electrodes at the exit and inlet $\partial\psi/\partial Z=\partial\omega/\partial Z=0$ [15]. We need to interpret this in terms of the velocity components.

$$\partial\psi/\partial Z=0\Rightarrow V=0\ at\ Z\pm z_0/r_0\Rightarrow V_{2,j}=V_{m,j}\ \ j=2,3,....n-1 \qquad (6a)$$

For the U velocity component we differentiate the above condition with respect to R

$$\partial/\partial R\left(\partial\psi/\partial Z\right)=\partial/\partial Z\left(\partial\psi/\partial R\right)=\partial/\partial Z\left(RU\right)=R\,\partial U/\partial Z$$
$$R\partial U/\partial Z=0\Rightarrow\partial U/\partial Z=0;\Rightarrow\left(\partial U/\partial Z\right)_{2,j}=\left(\partial U/\partial Z\right)_{m,j} \qquad (6b)$$

The second condition at the wall, $\partial\Omega/\partial Z=0$ can also be written in terms of the velocity components by noting that equation (5b) can be expressed as:

$$\omega=1/R\left(R\partial U/\partial R-U-R\partial V/\partial Z\right) \qquad (6c)$$

Hence

$$\partial\omega/\partial Z=1/R\left(\partial/\partial Z\left\{R\,\partial U/\partial R\right\}-\partial U/\partial Z-R\left\{\partial^2V/\partial Z^2\right\}\right)=0$$
$$\partial\omega/\partial Z=R\left(\frac{\partial^2V}{\partial Z^2}\right)=0\Rightarrow\left(\frac{\partial^2V}{\partial Z^2}\right)_{2,j}=\left(\frac{\partial^2V}{\partial Z^2}\right)_{m,j}=0 \qquad (6d)$$

Equations (6a) to (6d) are approximated by finite differences to read

$$U_{1,j}=U_{3,j}\ \ for\ LHS\ BC\ and\ U_{m+1,j}=U_{m-1,j}\ \ for\ RHS\ BC \qquad (6e)$$

$$V_{1,j}=-V_{3,j}\ \ for\ LHS\ BC\ and\ V_{m+1,j}=-V_{m-1,j}\ \ for\ RHS\ BC \qquad (6f)$$

Vorticity distribution is computed from equation (5d). Along the tube axis and the walls vorticity is set to zero except at the exit, except at the inlet and the exit where the zero gradient specification leads to a finite difference approximation expressed as

$$\omega_{1,j} = \omega_{3,j}, and \quad \omega_{m+1,j} = \omega_{m-1,j} \qquad (6g)$$

RESULTS AND DISCUSIONS

Fig.2 shows the profile of an electric current through an orifice in the presence of a conducting fluid. The electric current converges at the central electrode where higher R**B** values are registered. This is in agreement with the specified boundary conditions as well as the fact that the tube walls are non-conducting.The central electrode discharges towards the inlet and the exit, and produces an axisymmetrical configuration of the current streamlines. Electromagnetic forces result in this process, and are vital in the modification of the flow of fluid through the tube.

Fig.3 is the profile of the electromagnetic force field. The rotational electromagnetic force associated with the current is displayed as two oppositely revolving force fields. These forces are rotational, and are not balanced by body forces arising from pressure gradient unless at steady state. This imbalance gives rise to acceleration that impact on the dynamical features of the conducting fluid.

Rotational forces will most likely develop secondary flows when the vorticity production becomes appreciable. It can be observed from Fig. 4 that secondary flow is initiated in the region starting from the tip of the orifice and towards the upper wall at t= 10 for C = 0.3 and for a Reynolds number value of 100. Fig. 4 also depicts the axial velocity profiles of descending magnitude as the upper boundary wall is approached. A zero velocity value corresponds to the position of the upper lip of the aperture. As the flow enters and exits through the orifices, it impacts the solid boundaries at the inlet and exit. This results in a flow reversal which is indicated in the magnitude of the velocity values in this vicinity.

Fig. 5a displays the vorticity field generated with ζ given as 0.3 and Reynolds number of 50 at a time of 2.5. As the fluid enters the orifice, and makes the first impact with the lip of the orifice, vorticity is generated along the solid wall leading to the upper boundary. We observe an increase of vorticity away from the wall in the axial direction. At this point in time , there is more vorticity generation at the upstream of the central electrode than in the downstream as the hydrodynamic effects of the fluid contact with the orifice has not been sufficiently felt downstream. Fig. 5b displays the vorticity field at a later time (t=5). The impact of the vorticity produced by the central electrode is observed as the fluid moves towards the exit. In addition contributions from both the solid walls and electromagnetic field are merged, with those of the central electrode. The overall picture , indicates that more vorticity is produced closer to the walls and in the vicinity of the central electrode.

In the second experiment, it is found that the strength of the magnetic field as indicated by the magnetic pressure number and the size area of the electrode in the middle of the nonconducting tube introduce some vital electromagnetic effects that produce different flow patterns. This is demonstrated by the flow streamline patterns along the tube axis (Figs. 6a and 6b). The increase

in the gradient of the streamlines over the central electrode with respect to the radial coordinate indicates an increase of the axial velocity. As a fact , flows of this kind mimic those of ordinary flows when they encounter solid bodies as can be seen for flows past a plate aligned normal to the freestream direction. However one thing that needs to be pointed out in this case is that there is a continuous decrease in flow as it moves towards the current constriction created by the central electrode(Figs 7a and 7b). Minimum speed is observed just before the central electrode as shown by the axial velocity profile at the tube's centerline. However in order to satisfy continuity requirements, the flow accelerates to speeds higher than the entry speed and having made up for the continuity of mass, it decelerates once again to the speed of entry. This occurrence is noticeable as the value of the magnetic pressure number ζ is increased. It is worthwhile to note that nonuniformities in the flow electromagnetic field enhance their interaction with the dynamics of a conducting fluid and the eventual generation of Lorenz forces which are basically damping in nature. Figure 7b shows that as the electromagnetic pressure number is increased, the flow becomes dispossessed of enough kinetic energy to flow over the pressure hump created by the central electrode. This is shown by how far below zero the tube's axial velocity goes just before it gets to the central electrode.

The presence of negative values of axial velocity before the approach to the central electrode is indicative of the formation of secondary flows. These observations show in a simple manner how the Lorenz force acts as an impediment to flow and as a consequence generates vorticity and secondary flows. The value of ζ plays a significant role in flow configuration . For relatively small values of ζ , the flow is only slightly deviated from its oncoming direction towards the central electrode, while an increase in ζ creates stagnation zones in front of the central electrode. Figs. 8a and 8b show that for $\zeta = 0.8$, counter-rotating vortices appears in the region of the central electrode. Both diagrams also show that the diffusive-convective transport of vorticity involves a considerable portion of the flow domain both upstream and downstream of the central electrode.

The so called 'pinch effect' in the vicinity of the obstacle (central electrode) is indicative of a non-smooth transition. It offers a region of intense hydrodynamic activity as illustrated by a deficit in the fluid axial velocity(Figs. 9a and 9b) and a consequential build up of velocity in the radial direction (Figs. 10a and 10b). Figure 11 shows that near the central electrode, the current streamlines are distributed uniformly and directed towards the negative radial direction before it arrives at the obstacle. This shows that the Lorentz force opposes fluid motion in this region and as a result causes its deviation from the streamwise direction and reverses this direction immediately after the obstacle.

CONCLUSION

Most of the flows found in scientific literature dealing with nonuniform magnetic fields are related to the magnetohydrodynamics of duct flows in the streamwise direction arising from the

interaction of electric and magnetic fields[16,17,18]. The current study in addition to this, examines the variations arising from orifice flow exposed to an electromagnetic field. In all cases this study has further illustrated how the Lorentz force produced by the interaction of electric and magnetic fields slows down the flow and generates vorticity. This may be of practical importance where mixing or heat enhancement is needed. The governing continuum equations that comprise the balance laws of mass and momentum are modified to include the electromagnetic effects. These have been solved numerically using the finite difference methods. The correctness of the numerical algorithm developed herein was confirmed by noting the closeness of some of the results with those from literature(Chow[15]). It is hoped that this work will help in further understanding of flows produced by localized forces and nonuniform magnetic fields and their concomitant effects in providing mixing, vorticity and heat enhancement.

REFERENCES

1. Chow C-Y and Uberoi, M.S. Secondary flows due to axisymmetric converging-diverging electric current, Computers and Fluids 6 (1978) 115

2. Uberoi, M.S. Magnetohyerodynamics at small magnetic Reynolds numbers, Phys. Fluids 5, (1962) 401

3. Narain, J.P. and Uberoi, M.S. Magnetohydroynamics of conical flows, Phys. Fluids 14 (1971) 14

4. Shercliff, J.A. The flow of conducting fluids in circular pipes under transverse magnetic f ields J. Fluid Mech 1 (1956) 644

5. Di Piazza, I and Buhler, A general computational approach for magnetohydrodynmic flows using CFX code: buoyant flow though through a vertical square channel, Fusion Technology, 38 (2000) 180

6. Uberoi, M. S, and Chow , C-Y. Large scale motions in electrical discharges, Phys. Fuid 20 (1977) 1815

7. Ritter, J.M. Two phase fluid flows in pipes and channels. M.S. Thesis, Tennessee Technological Society 1976

8. Chamkha, A.J. Unsteady laminar hydromagnetic fluid-particle flow and heat transfer in channels and circular pipes, Int. Jnl. Heat and Fluid Flow 21 (2000) 740

9. Chamkha, A.J. Hydromagnetic two-phase flow in a channel. Int. Jnl. Engnr. Sci. 33 (1995a) 437

10. Chamkha, A.J. Time dependent two-phase channel flow due to an oscillating pressure gradient. Fluid/Particle Separation Jnl.8, (1995b) 203

11. Onyejekwe, O.O. Magnetohydrodynamics flow in a tube with centrally placed electrodes. Int. Comm. Heat and Mass Transf. 35, (2008) 1241

12. Pantokratoras, A. Some new parallel flows in weakly conducting fluids with an exponenetially decaying Lorentz force. Math. Probl. in Engnr. 2, (2007) 1

13. Kabbani, H.S. Martin J.M. Joo, S.W. Qian S Analytical prediction of flow in magnetohydrodynamic fluidic devices, 130 (2008) 1

14. Soundalgekar, V.M. Finite difference analysis of transient free convection with mass transfer on an isothermal vertical flat plate, Int. Jnl. Engnr. Sci. 19 (1981) 757

15. Chow, C-Y An introduction to computational fluid mechanics. Publishers: John Wiley and sons 1979 396 pages

16. Altinas, A. and Ozkol I. Magnetohydrodynamic flow of liquid-metal in circular pipes for externally heated non heated cases, Jnl. Appld. Fluid Mech. 8(2015) 507

17. Jing, Z. M.-J. Ni, and Z.-H Wang Numerical study of MHD natural convection of liquid metal with wall effects, Num. Heat Transfer 6 (2013) 563

18. Rao, J.A., Raju, R.S., and Sivsiah S., Finite element solution of heat and mass transfer in MHD flow of a viscous fluid past a vertical plate under oscillatory suction velocity,Jnl. Appld. Fluid Mech. 5 (2012) 1

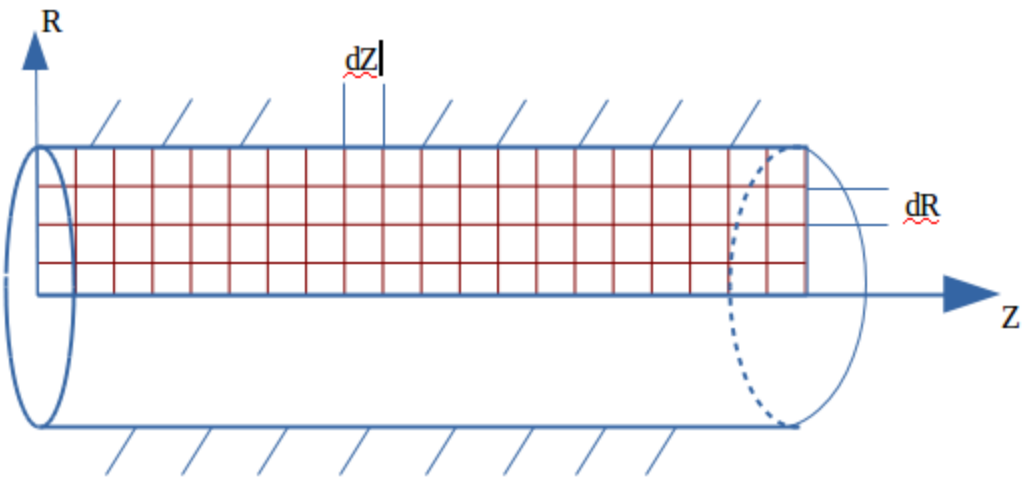
R
dZ
dR
Z

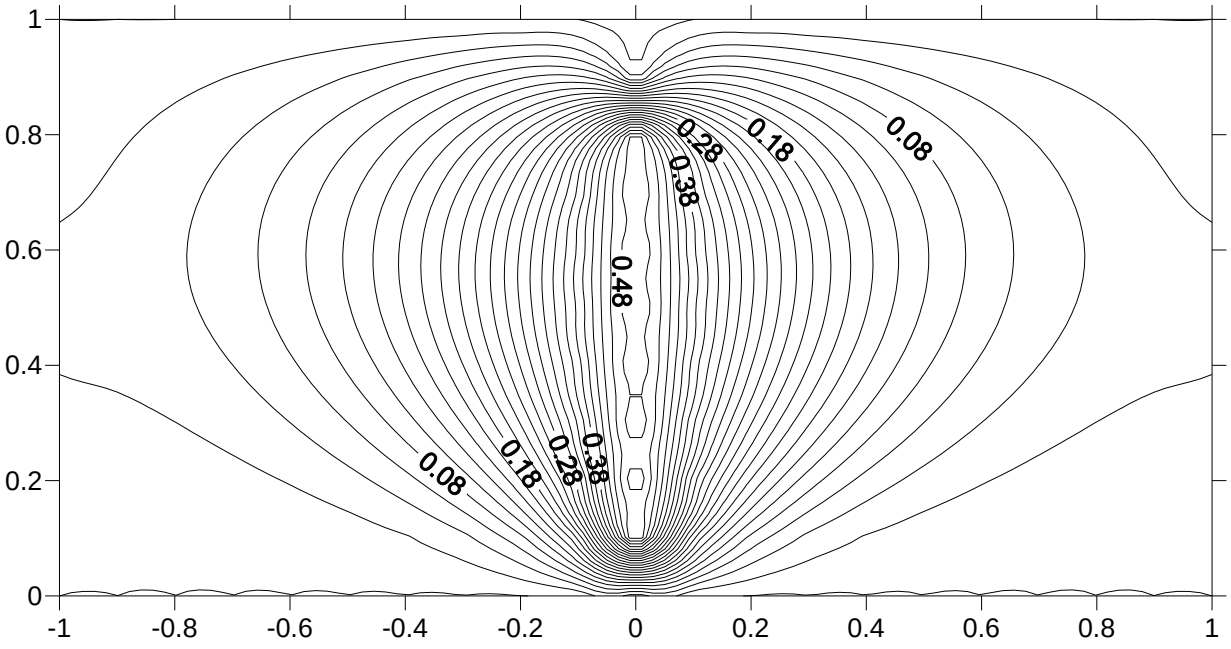
1
0.8
0.6
0.4
0.2
0
-1
-0.8
-0.6
-0.4
-0.2
0
0.2
0.4
0.6
0.8
1
0.08
0.18
0.28
0.38
0.48
0.38
0.28
0.18
0.08

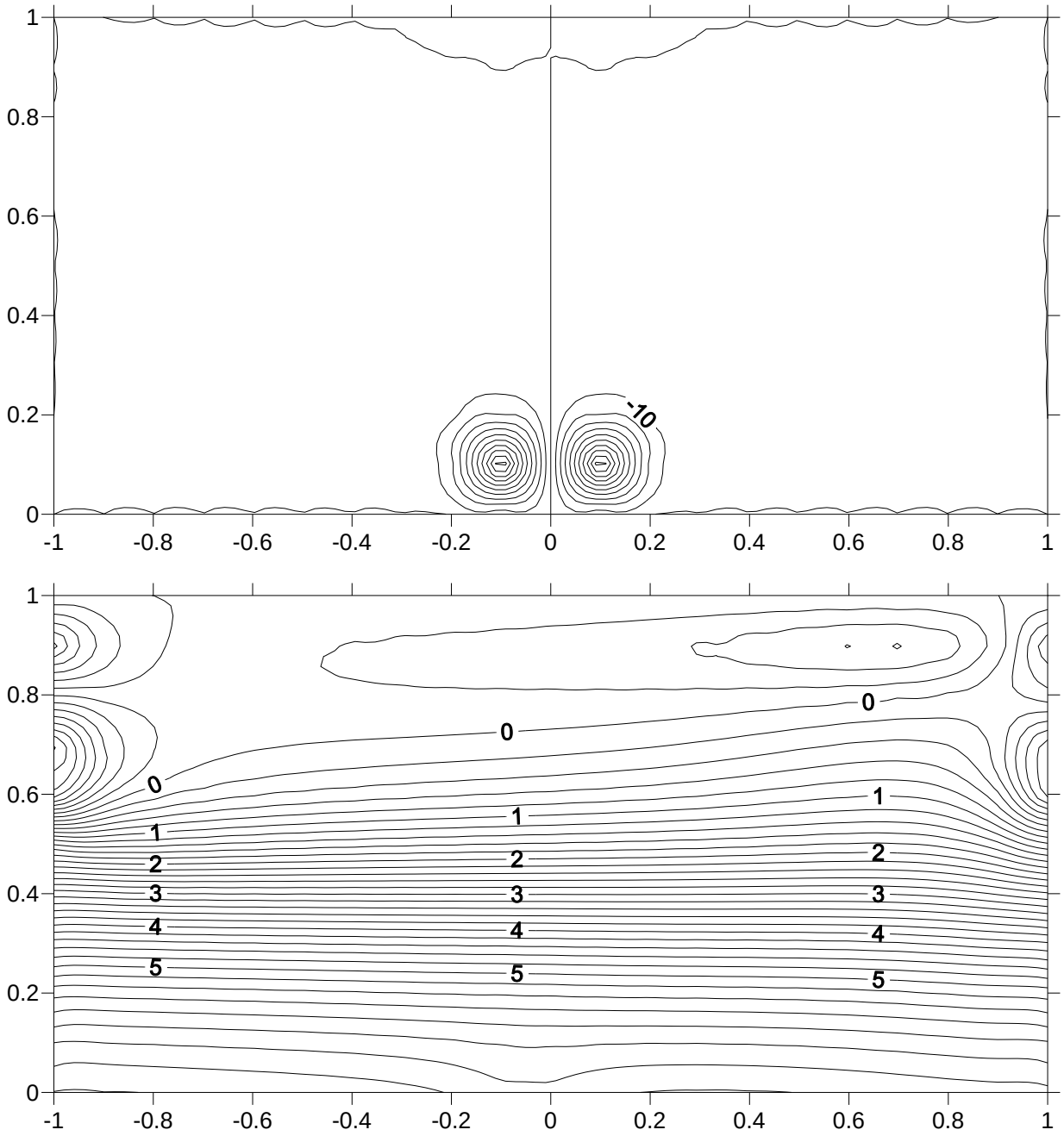
1
0.8
0.6
0.4
0.2
0
-1
-0.8
-0.6
-0.4
-0.2
0
0.2
0.4
0.6
0.8
1
-10
0
1
2
3
4
5

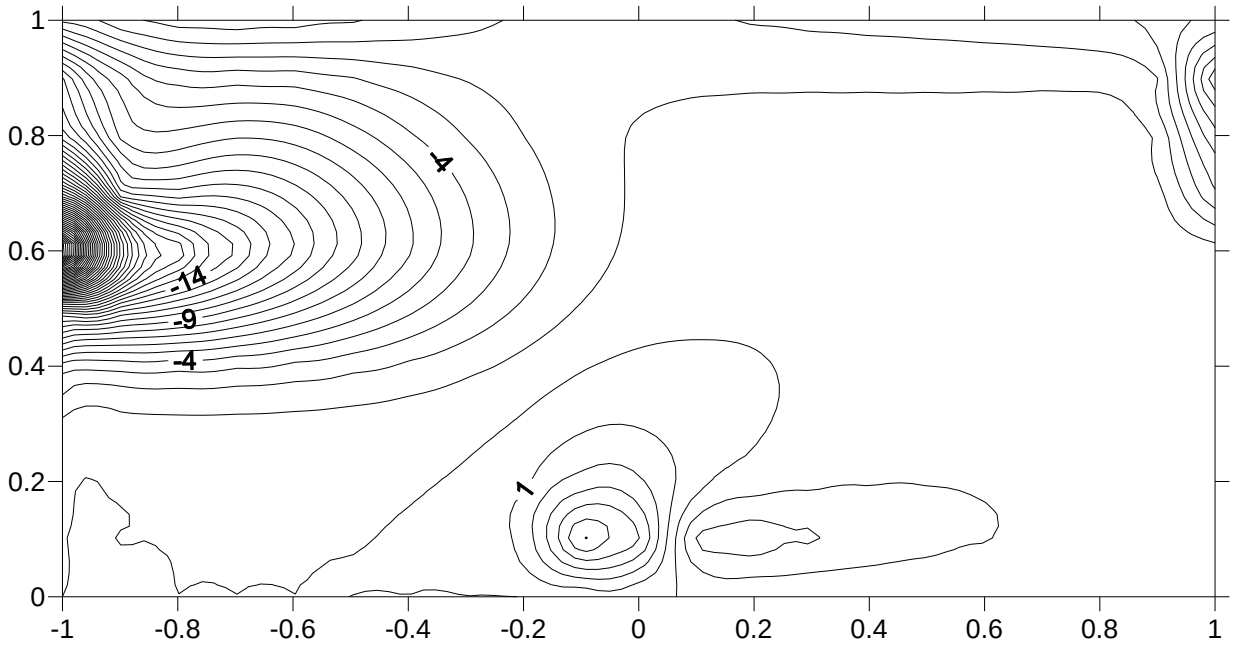
1
0.8
0.6
0.4
0.2
0
-1
-0.8
-0.6
-0.4
-0.2
0
0.2
0.4
0.6
0.8
1
4
-14
-9
-4
1

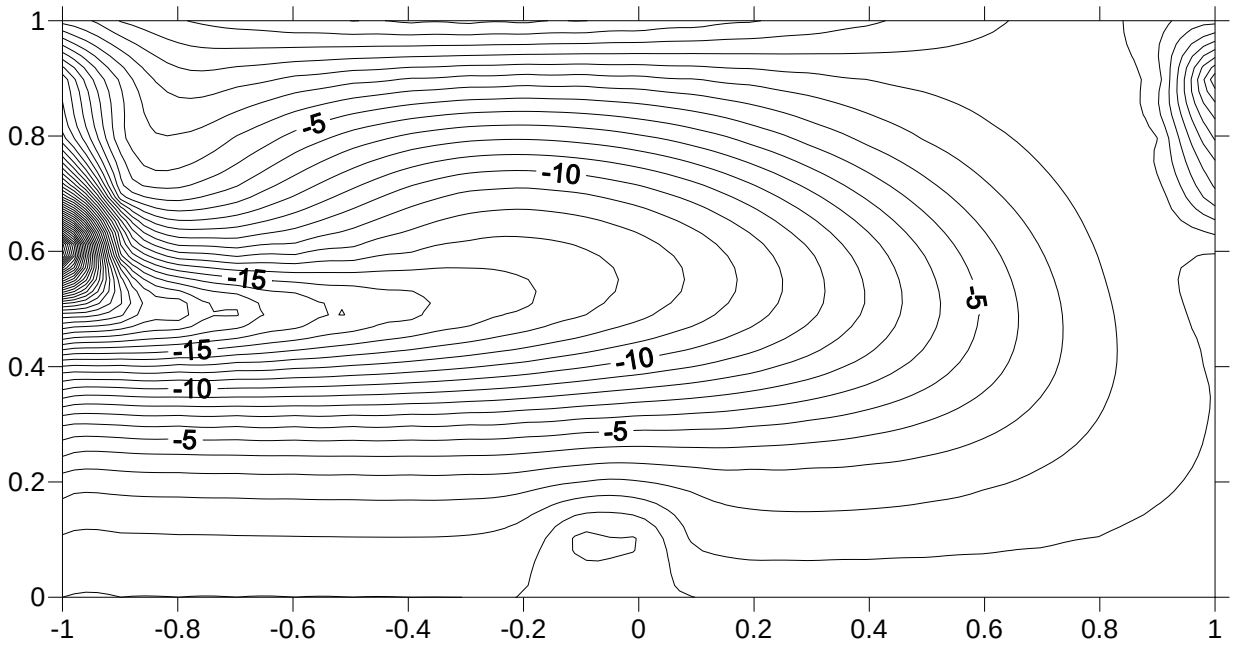
1
0.8
0.6
0.4
0.2
0
-1
-0.8
-0.6
-0.4
-0.2
0
0.2
0.4
0.6
0.8
1
-5
-10
-15
-15
-10
-5
-10
-5
5

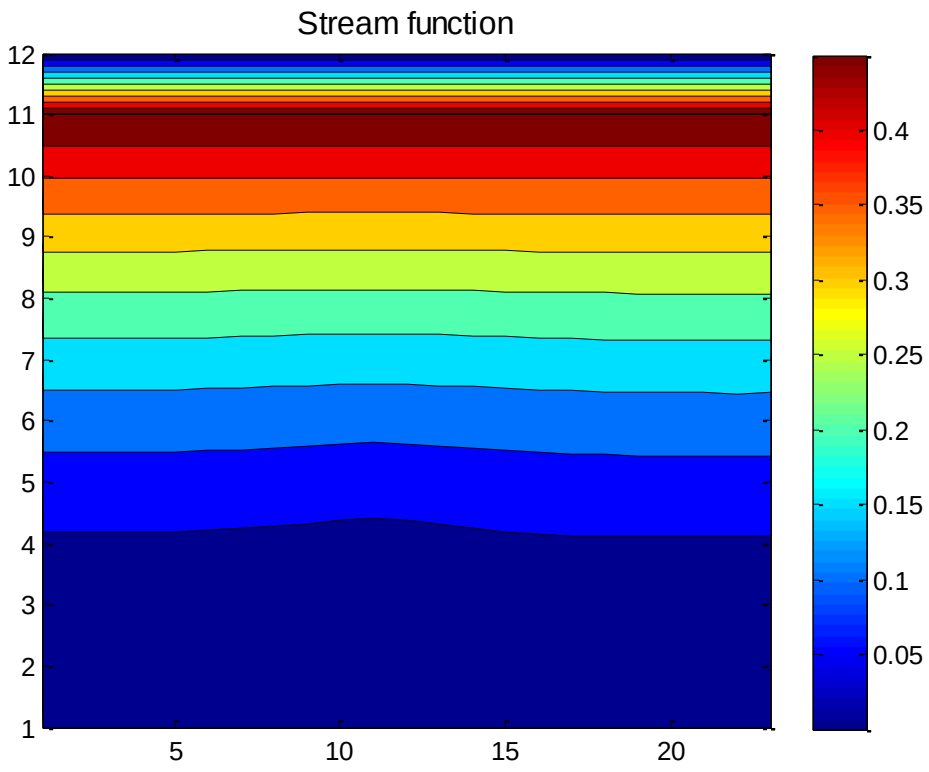
Stream function
12
11
10
9
8
7
6
5
4
3
2
1
5
10
15
20
0.4
0.35
0.3
0.25
0.2
0.15
0.1
0.05

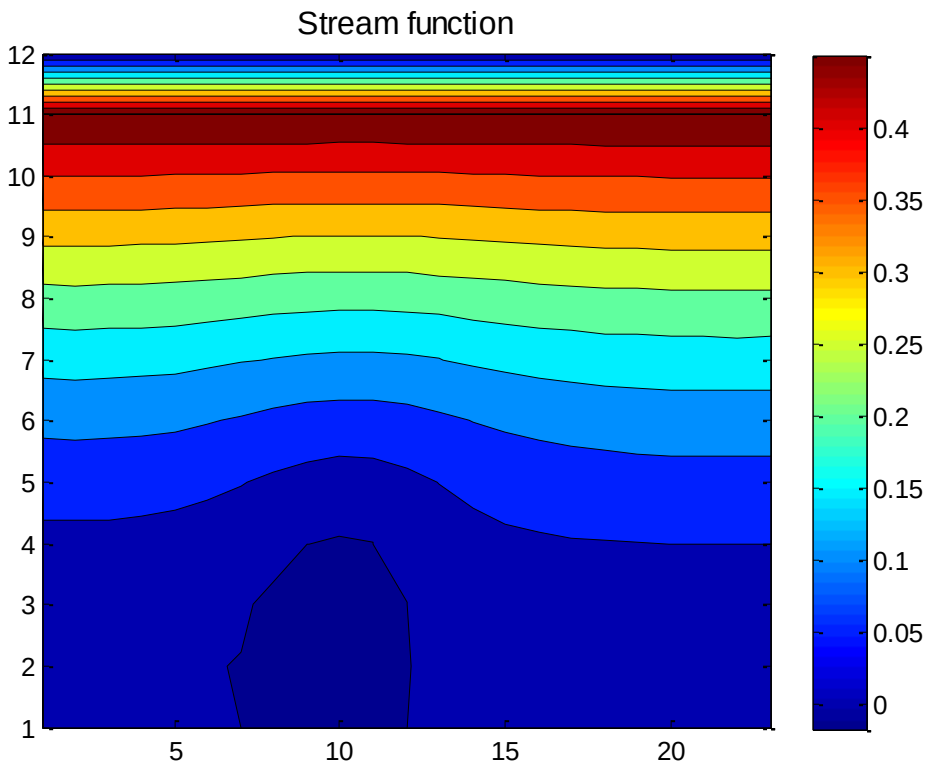
Stream function
12
11
10
9
8
7
6
5
4
3
2
1
5
10
15
20
0.4
0.35
0.3
0.25
0.2
0.15
0.1
0.05
0

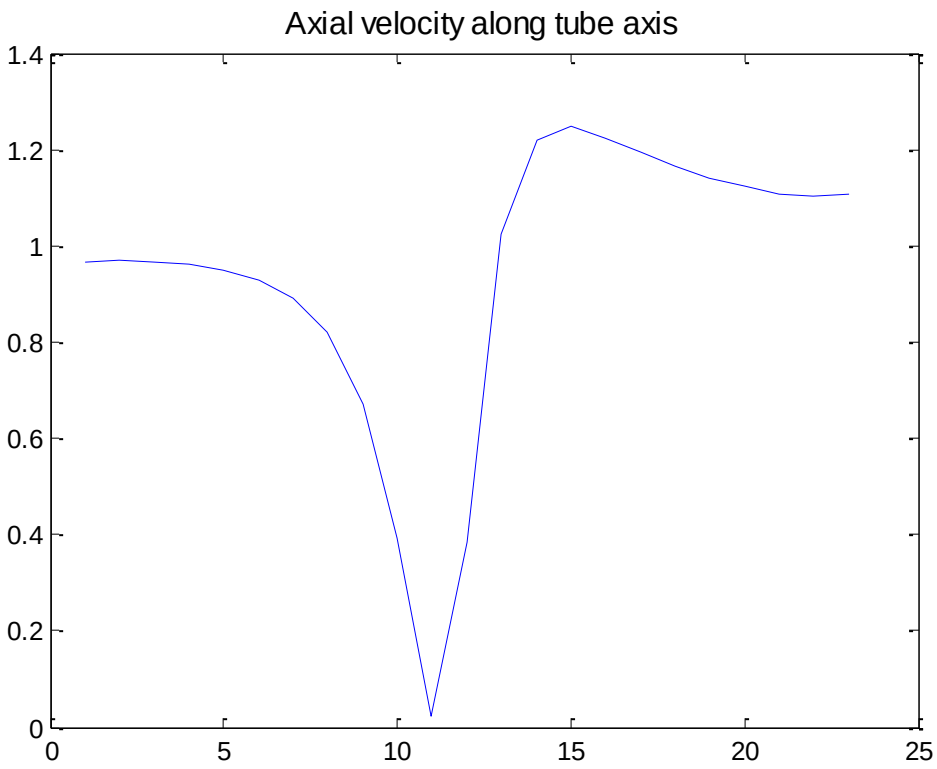
Axial velocity along tube axis
1.4
1.2
1
0.8
0.6
0.4
0.2
0
0
5
10
15
20
25

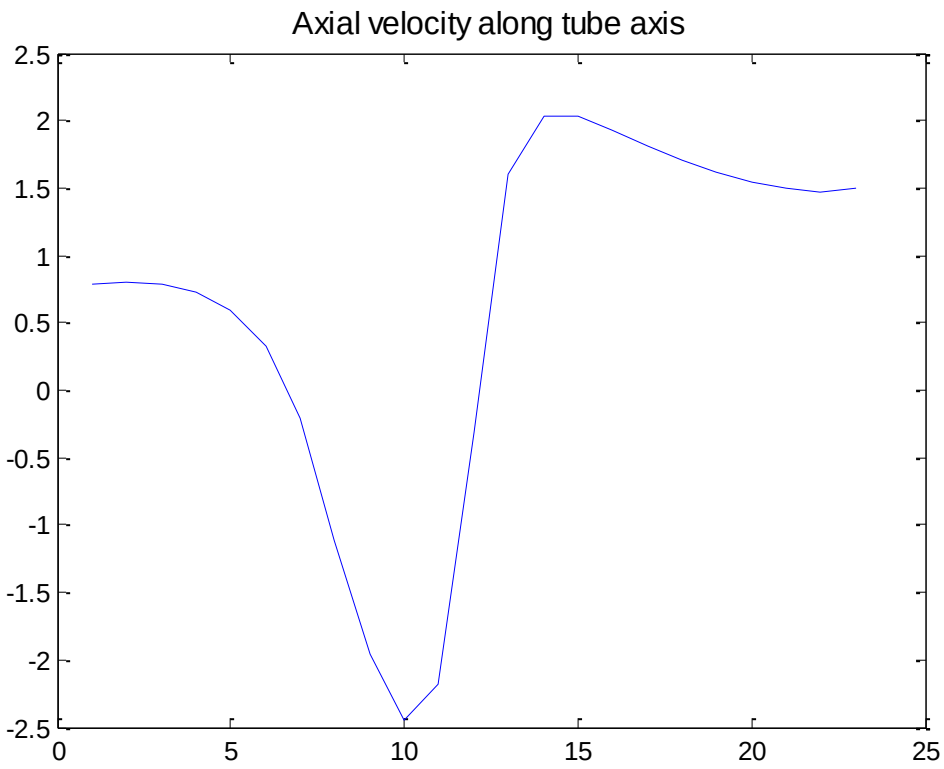
Axial velocity along tube axis
2.5
2
1.5
1
0.5
0
-0.5
-1
-1.5
-2
-2.5
0
5
10
15
20
25

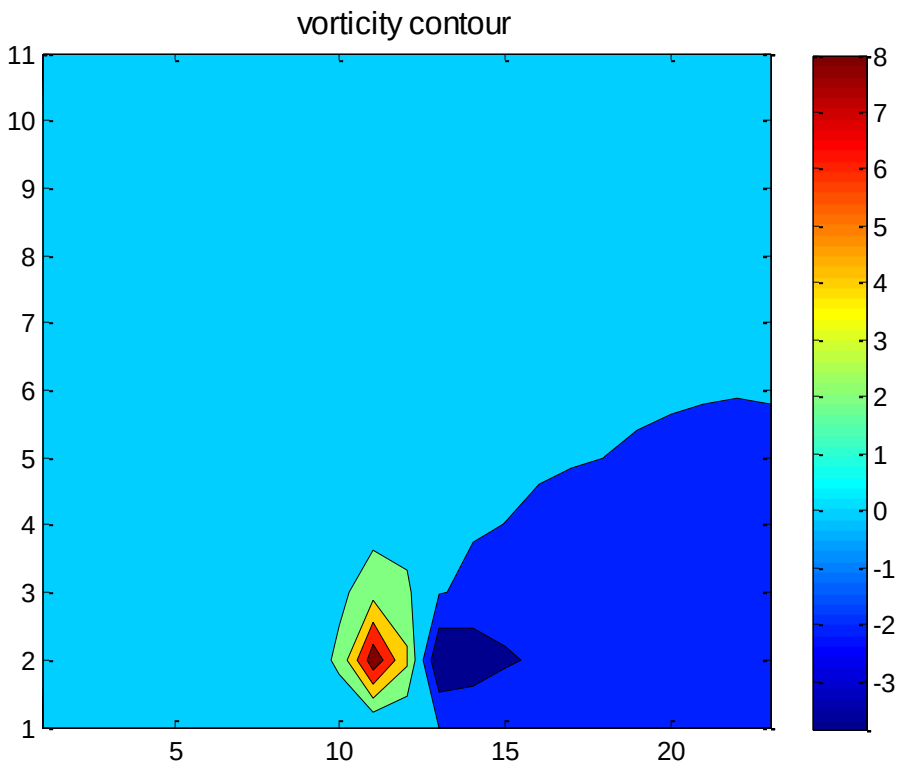
vorticity contour
11
10
9
8
7
6
5
4
3
2
1
5
10
15
20
8
7
6
5
4
3
2
1
0
-1
-2
-3

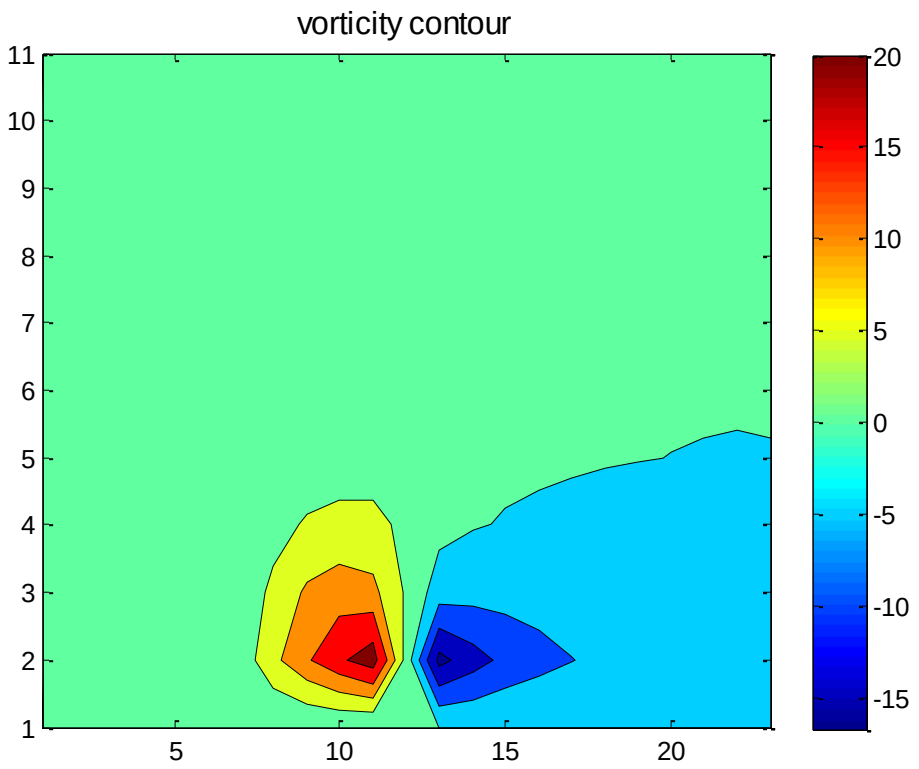
vorticity contour
11
10
9
8
7
6
5
4
3
2
1
5
10
15
20
20
15
10
5
0
-5
-10
-15

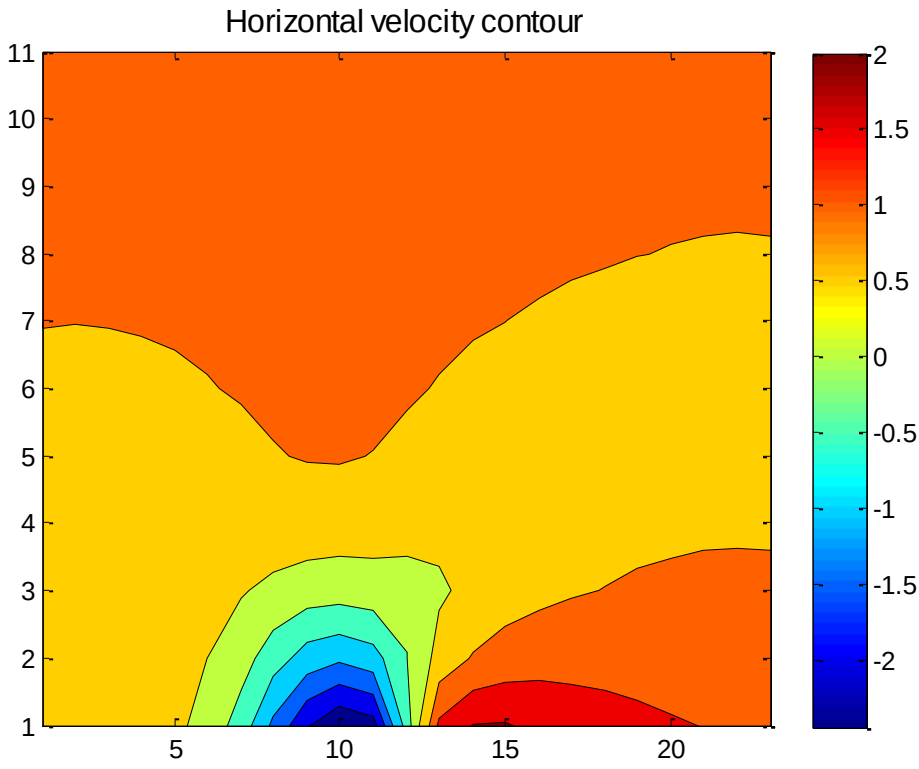
Horizontal velocity contour
11
10
9
8
7
6
5
4
3
2
1
5
10
15
20
2
1.5
1
0.5
0
-0.5
-1
-1.5
-2

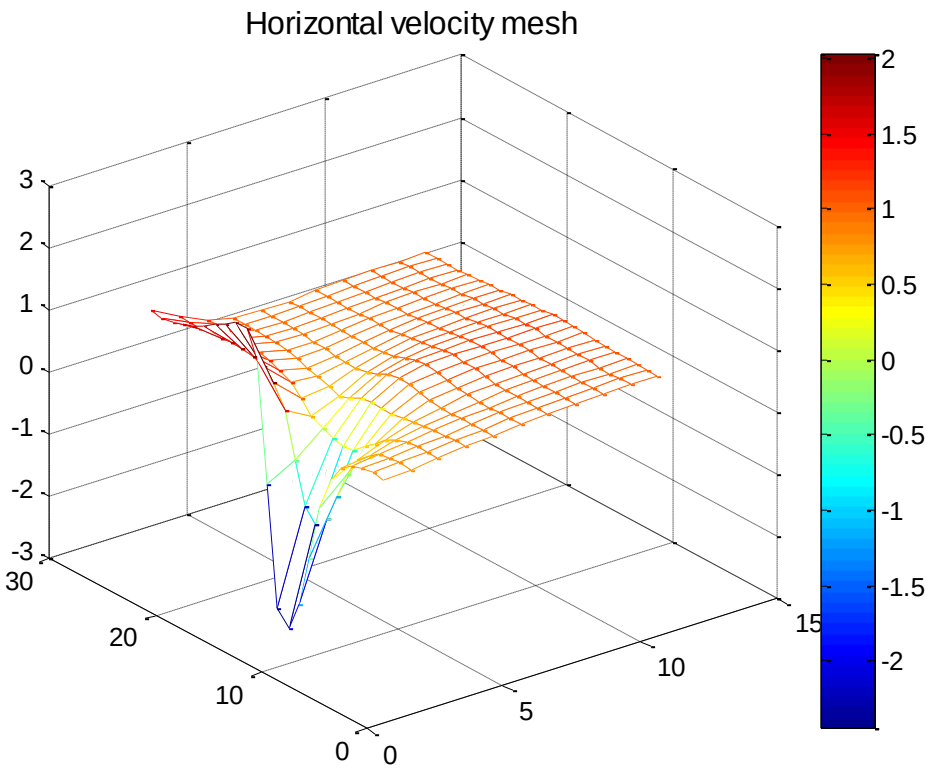
Horizontal velocity mesh
3
2
1
0
-1
-2
-3
30
20
10
0
0
5
10
15
2
1.5
1
0.5
0
-0.5
-1
-1.5
-2

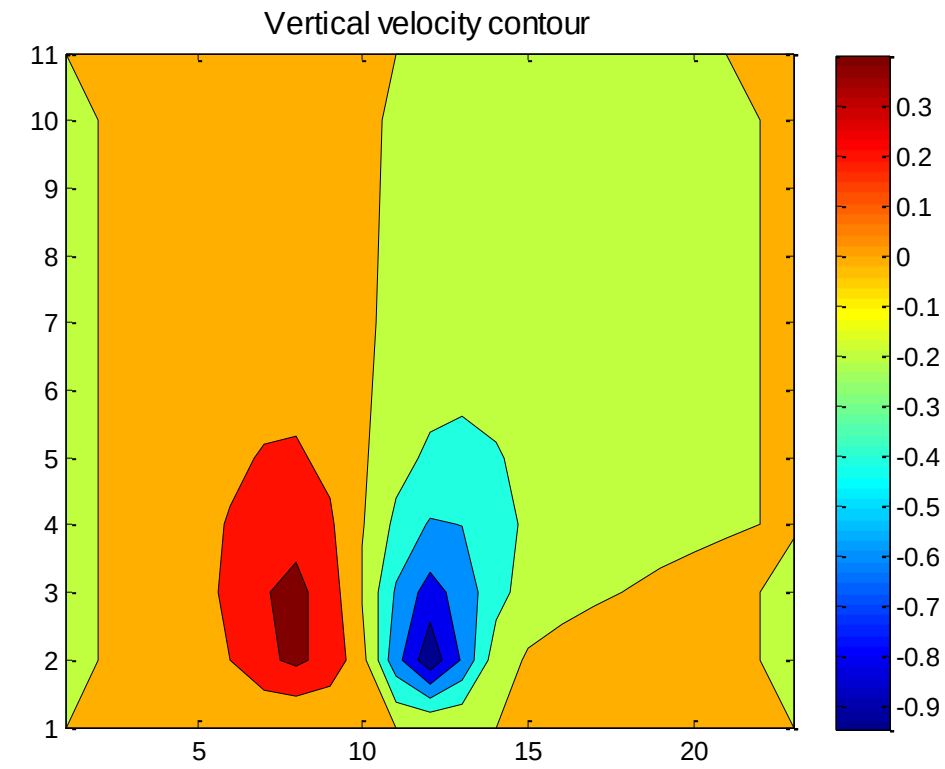
Vertical velocity contour
11
10
9
8
7
6
5
4
3
2
1
5
10
15
20
0.3
0.2
0.1
0
-0.1
-0.2
-0.3
-0.4
-0.5
-0.6
-0.7
-0.8
-0.9

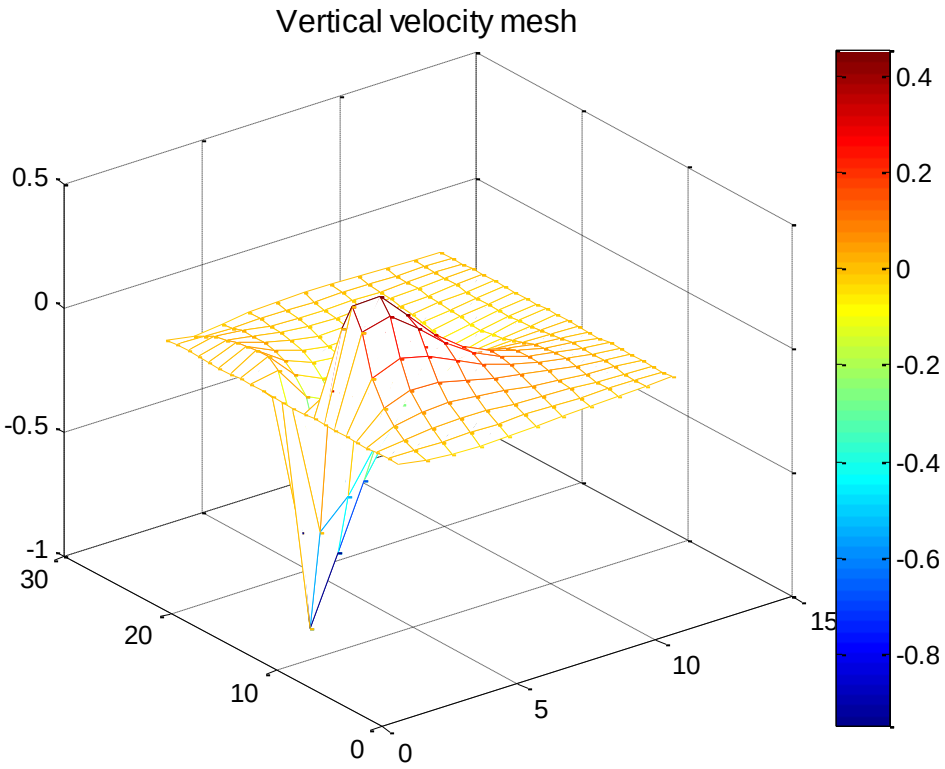
Vertical velocity mesh
0.5
0
-0.5
-1
30
20
10
0
0
5
10
15
0.4
0.2
0
-0.2
-0.4
-0.6
-0.8

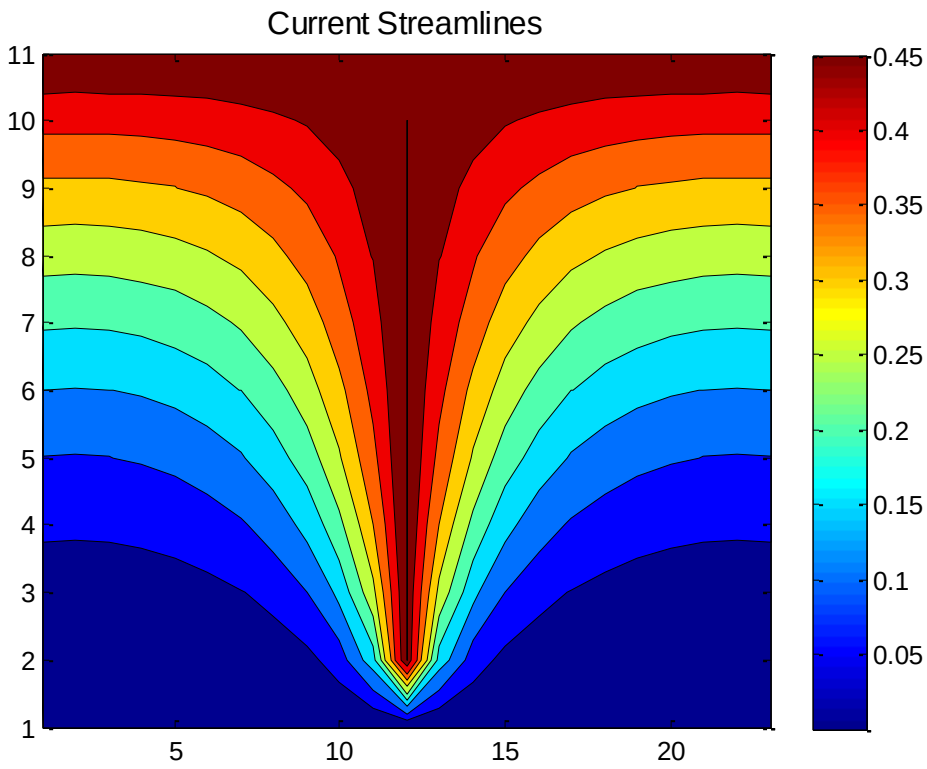
Current Streamlines
11
10
9
8
7
6
5
4
3
2
1
5
10
15
20
0.45
0.4
0.35
0.3
0.25
0.2
0.15
0.1
0.05

List of figures